Investigating Amorphous Order in Stable Glasses by Random Pinning

Christopher J. Fullerton and Robert L. Jack
Department of Physics, University of Bath, Bath BA2 7AY, United Kingdom
(Received 4 December 2013; published 27 June 2014)

We investigate stable glassy states that are found when glass-forming liquids are biased to lower than average dynamical activity. By pinning the positions of randomly chosen particles, we show that many-body correlations in these states are relatively strong and long ranged compared to equilibrium reference states. The presence of strong many-body correlations in these apparently disordered systems supports the idea that stable glassy states exhibit a kind of "amorphous order," which helps to explain their stability.

DOI: 10.1103/PhysRevLett.112.255701 PACS numbers: 64.70.Q-, 05.40.-a, 61.20.Ja

Glassy materials are stable and appear to be solid, but their molecular structures closely resemble those of liquids [1,2]. Reconciling these two observations is a central challenge if the properties of these important materials are to be understood. To this end, a useful concept is amorphous order, which means that while the structure of a glass appears highly disordered, there may, nevertheless, be strong correlations between particles, extending over significant length scales [3–5], and leading to glassy behavior [3,6,7]. These correlations can be revealed through a system's response to pinning multiple particles in place, with the others left free to relax [8–12]. Alternatively, instead of searching for some kind of order in the configurations of a glassy system, one may take a dynamic approach [13,14], focussing on the trajectories by which these systems evolve in time. By concentrating on trajectories with lower than average dynamic activity, recent studies have revealed nonequilibrium phase transitions [15–18] and unusually stable glassy states [19]. Here, we use random pinning measurements [10–12] to show that while these stable states were found by analyzing their dynamical properties, they also exhibit strong amorphous order. We argue that these results offer a point of contact [20,21] between the dynamicawsml approach based on low-activity trajectories [15,16] and structural approaches based on amorphous order [3–7].

We consider the well-studied glass-forming liquid of Kob and Andersen [22]. This system exhibits a nonequilibrium "inactive phase" [16], which is extremely stable [19] and is found by biasing dynamical trajectories to low activity. The stable glassy states that we consider were taken from this inactive phase [23], for a system of $N = 150$ particles [24]. The unit of length in this system is the diameter σ of the larger particles (type A), the system size is $L = 5\sigma$, and all results shown are for temperature $T = 0.6$ (in units of the AA-interaction energy), for which the equilibrium state is a weakly supercooled fluid. The system evolves by overdamped (Monte Carlo) dynamics [28], which gives results for structural relaxation in quantitative agreement with molecular dynamics [16,28]. Time is measured in units of $\Delta t = \sigma^2/D_0$, where D_0 is the diffusion constant of a free particle.

To analyze amorphous order in inactive states, we use a random pinning procedure [10,11]. For a given reference configuration, we fix the position of each particle with probability c, arriving at a "template": a set of approximately cN pinned particles. The remaining (unpinned) particles then move as normal in the presence of the frozen template. If the reference configuration is highly ordered, one expects a strong influence of the template on the resulting system. For example, in a perfectly crystalline sample, a template containing just three particles is sufficient to determine the lattice orientation and, hence, the positions of all other particles. More generally, if a template containing a small fraction of particles has a strong influence on the liquid structure, this indicates that the correlations among particle positions are strong, and hence that the system is ordered, even if this order is not apparent from two-point density correlations.

To analyze the influence of the template, we require a measure of similarity between configurations. To account for configurations where particle indices are permuted but the structure remains similar, we divide the system into a cubic grid of cells of size $\ell = (L/10) = 0.5\sigma$ [10]. Let n_i be the number of mobile (unpinned) particles of type A in cell i. Then, if configurations $\mathcal{C}$ and $\mathcal{C}'$ have cell occupancies $\{n_i\}$ and $\{n_i'\}$, their overlap is

$$Q(\mathcal{C},\mathcal{C}') = \frac{1}{M}\sum_i \frac{n_i n_i' - \langle n_i\rangle^2}{\langle n_i^2\rangle - \langle n_i\rangle^2}. \quad (1)$$

If $\mathcal{C}$ and $\mathcal{C}'$ are identical then $\langle Q\rangle = 1$ while, for independent random configurations, $\langle Q\rangle = 0$. While Q depends only on type-A particles, our results are very similar if the overlap is modified to include all particles [24].

For pinning from equilibrium states [10–12,29–36], a reference configuration $\mathcal{C}_0$ is drawn from an equilibrium distribution. We pin each particle in $\mathcal{C}_0$ with probability c (pinning a fixed number of particles [10,12,35] has similar effects [24]). Then, a second configuration $\mathcal{C}$ is generated,

which includes the pinned particles from $\mathcal{C}_0$, while the remaining particles are equilibrated in the presence of this template. Repeating this procedure many times, we build up a distribution $p_{\rm eq}(Q|c)$ for the overlap $Q = Q(\mathcal{C}_0, \mathcal{C})$. Note that this is a static (thermodynamic) procedure, in that $p_{\rm eq}(Q|c)$ depends only on the system's Boltzmann distribution [24].

To study inactive states, we draw reference configurations $\mathcal{C}_0$ from trajectories of the model that are biased to lower than average dynamical activity [24]. Starting from inactive reference configurations, we repeat the pinning procedure, which results in a different distribution of the overlap, denoted by $p_{\rm in}(Q|c)$. The inactive state is coupled to a thermostat at $T = 0.6$, so we compare the inactive state with an equilibrium state at that temperature. Differences in amorphous order between inactive and equilibrium states are reflected in differences between $p_{\rm eq}(Q|c)$ and $p_{\rm in}(Q|c)$.

To estimate these distributions, we conducted dynamical simulations. For a given reference configuration $\mathcal{C}_0$ and a given template, dynamical trajectories starting from $\mathcal{C}_0$ were used to calculate time-dependent overlaps $Q(\mathcal{C}_0, \mathcal{C}_t)$, where $\mathcal{C}_t$ is the configuration of the system at time t. This procedure is repeated for many different templates and different reference configurations. Figure 1(a) shows the time-dependent average overlap $C(t) = \langle Q(\mathcal{C}_0, \mathcal{C}_t)\rangle$, for both equilibrium and inactive reference configurations. The dynamical relaxation from inactive states is much slower than equilibrium relaxation, even in the absence of pinning [19]. Also, as c is increased, the dynamical relaxation slows down, for both equilibrium and inactive reference states [10,36].

Figures 1(b) and 1(c) indicate that the slow decay of $C(t)$ is associated with large fluctuations of $Q(\mathcal{C}_0, \mathcal{C}_t)$. For long times, the time-dependent distribution $p^0_{\rm in}(Q|t, c)$ of this overlap has a characteristic bimodal shape. In contrast, the distribution $p^0_{\rm eq}(Q|t, c)$, obtained under the same conditions, lacks the second peak at high Q. The differences between these distributions are entirely due to the to the structural differences between the reference states (inactive or equilibrium) from which the pinned particles were selected. Further, the dynamics used here ensure [24] that $\lim_{t\to\infty} p^0_{\rm in}(Q|t, c) = p_{\rm in}(Q|c)$, so differences between the long-time limits of $p^0_{\rm in}(Q|t, c)$ and $p^0_{\rm eq}(Q|t, c)$ reflect differences between $p_{\rm eq}(Q|c)$ and $p_{\rm in}(Q|c)$. However, Fig. 1 shows that $p^0_{\rm in}(Q|t, c)$ has not reached its large-t limit, so we may not assume that the "dynamical" distribution $p^0_{\rm in}(Q|t, c)$ reflects the form of the "static" distribution of interest, $p_{\rm in}(Q|c)$. In particular, the large-Q peak in $p^0_{\rm in}(Q|t, c)$ might disappear on increasing t, as the system relaxes further.

We, therefore, conducted simulations in which a template was fixed as before, after which the temperature was increased to $T = 5.0$ and dynamics run for $t \approx 1000\Delta t$. This temperature is high enough that the mobile particles quickly decorrelate from their initial configuration. These

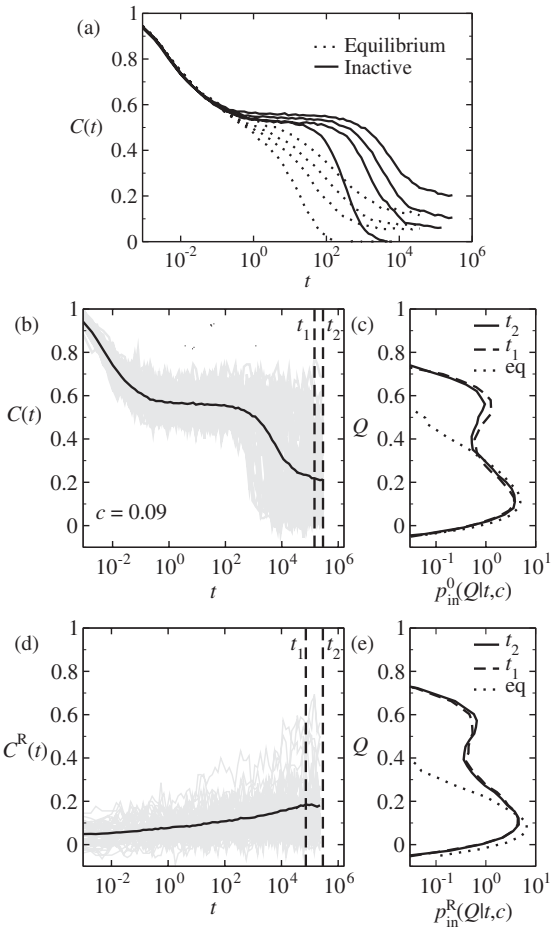

FIG. 1. (a) $C(t)$, calculated from equilibrium and inactive reference configurations. From left to right $c = 0.00, 0.05, 0.07, 0.09$. (b) For an inactive reference state and $c = 0.09$, the average overlap $C(t)$ (black) and plots of $Q(\mathcal{C}_0, \mathcal{C}_t)$ for representative trajectories (gray). (c) Distributions $p^0_{\rm inac}(Q|t, c)$ at the times indicated and $c = 0.09$, compared with $p^0_{\rm eq}(Q|t, c)$ for an equilibrium reference state, under the same conditions. (d),(e) Data analogous to (b),(c), but using initial configurations in which the positions of unpinned particles were randomized.

"randomized" states were then used as initial conditions for dynamical simulations (see also [8,37]). We again measured the distribution of the overlap between the reference $\mathcal{C}_0$ and the resulting time-dependent configurations $\mathcal{C}_t$. Let the distribution of this overlap be $p^{\rm R}_{\rm in}(Q|t, c)$ and let $C^{\rm R}(t) = \langle Q(\mathcal{C}_0, \mathcal{C}_t)\rangle$.

Results are shown in Figs. 1(d) and 1(e): the average overlap $C^{\rm R}(t)$ starts near zero (as expected for a randomized initial condition) and slowly increases, due to the influence of the template. For large times, there is a significant fraction of trajectories in which the system spontaneously evolves into a state with large Q. That is, the frozen template (containing just 9% of the particles) influences these trajectories so strongly that they return to the same metastable state as the original reference configuration. As before, $p^{\rm R}_{\rm in}(Q|t, c) \to p_{\rm in}(Q|c)$ as

$t \to \infty$, but this limit is not saturated. However, while $p^{\mathrm{R}}_{\mathrm{in}}(Q|t,c)$ and $p^{0}_{\mathrm{inac}}(Q|t,c)$ are converging to the same limit, they do so from opposite directions: the original simulations start in the reference state $\mathcal{C}_0$ and evolve away from it, while the randomized simulations start far from $\mathcal{C}_0$ and evolve back towards it. Thus, a natural conjecture is that these two distributions give (approximate) upper and lower bounds on the distribution $p_{\mathrm{in}}(Q|c)$.

Figure 2 collates the relevant distributions. Inactive reference configurations lead to bimodal distributions, while the distributions obtained from equilibrium reference configurations are unimodal, for pinning fractions up to $c = 0.11$. In the Supplemental Material (SM) [24], we show that the structures of high-Q and low-Q states are very similar (at the two-particle level), ruling out a simple structural origin for the bimodality in Figs. 2(a) and 2(b). The probability associated with the large-Q peak in $p_{\mathrm{in}}(Q|t,c)$ rises in a strongly nonlinear fashion, indicating the central role of many-body correlations [38].

To show how these numerical results are related to amorphous order, we build on previous work on fluctuations of the overlap [39–41], writing

$$p(Q|c) = e^{-N\beta V(Q,c)}, \tag{2}$$

where $V(Q,c)$ is an effective potential, as used in mean-field theories of the glass transition [39], generalized to include the effects of pinning. Within mean-field theories and below the onset temperature ($T_{\mathrm{o}} \approx 1$ for this model), one expects two peaks in $p(Q|c)$, as Q is varied, and, hence, two minima in $V(Q,c)$. These correspond to $\mathcal{C}$ and $\mathcal{C}_0$ being in the same metastable state (high Q), or in different states (low Q). As c is increased, one expects the low-Q peak to be reduced, because cases where $\mathcal{C}$ is in a different state from $\mathcal{C}_0$ are not typically consistent with the frozen template. Within random first-order transition theory [7], one additionally expects a phase transition at some critical concentration c [11,42], so that the high-Q peak of $p(Q|c)$ dominates the distribution for $c > c^*$, while the low-Q peak dominates for $c < c^*$.

If such phase transitions occur in randomly pinned systems, the distribution $P(Q|c)$ remains bimodal as the system size $N \to \infty$. Numerically, this can be established by finite-size scaling analysis [12], but the long time scales associated with inactive states mean that this is beyond the scope of this study. Nevertheless, the bimodal distributions $P(Q|c)$ and the associated nonconvex $V(Q,c)$ shown here imply the existence of strong many-body correlations in these systems. As we now explain, Fig. 2 indicates that the inactive state in this model has a structural correlation length ξ that is comparable with the system size $L = 5\sigma$.

To show this, we follow [40] in considering spatial fluctuations of the overlap. For the equilibrium reference state considered here, it is expected that spatial fluctuations prevent any phase transition [11,36]. Hence, within the framework of the renormalization group, one does not expect long-ranged order, but one does expect strong spatial fluctuations of the order parameter Q, with an associated correlation length ξ. The expected situation [40] is sketched in Fig. 3—it occurs (for example) in plaquette spin models [33], which have glassy dynamics and growing amorphous order at low temperatures [43,44]. Consider

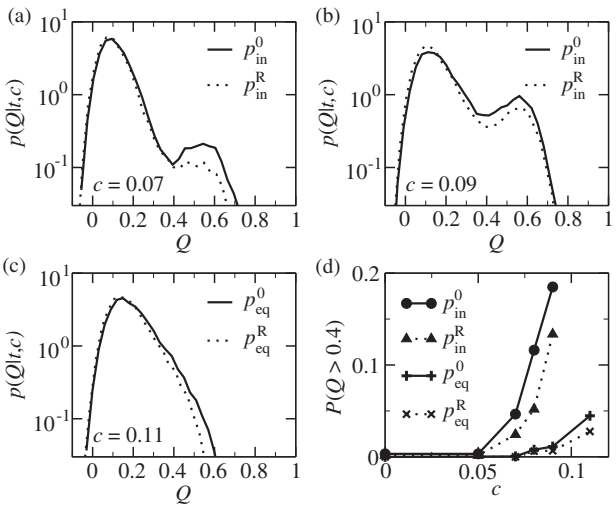

FIG. 2. (a)–(c) Distributions of $Q(\mathcal{C}_0, \mathcal{C}_t)$. (a) $c = 0.07$ for an inactive reference; (b) $c = 0.09$, inactive reference; (c) equilibrium reference, for $c = 0.11$ (results for lower c are similarly unimodal). In (b), $t = t_2$ as indicated in Fig. 1(b); for (a) and (c), the times are $3t_2/4$ and $t_2/4$, respectively. (d) Probabilities corresponding to the high-Q peak in the distributions $p(Q|t,c)$.

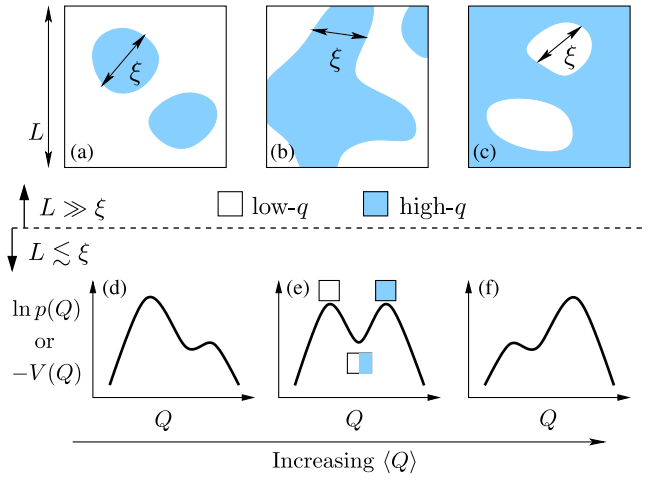

FIG. 3 (color online). (a)–(c) Sketches of the local overlap $q(\boldsymbol{r})$ within a large system ($L \gg \xi$), as $\langle Q \rangle$ increases. One expects [40] a domain structure of high-q and low-q patches, with an associated length scale ξ. (d)–(f) Sketches of distributions $\ln p(Q) = -N\beta V(Q)$ for small systems ($L \lesssim \xi$), under the same conditions as (a)–(c). For small systems, then, the domain structure leads to two peaks in $p(Q)$, with typical realizations of the system containing only one domain, as indicated in (e).

two configurations $\mathcal{C}$ and $\mathcal{C}'$ that share a template: shaded regions in Figs. 3(a)—3(c) indicate parts of the system where the overlap between $\mathcal{C}$ and $\mathcal{C}'$ is large. Specifically, we define a local overlap $q(\boldsymbol{r}, \mathcal{C}, \mathcal{C}')$ so that $Q(\mathcal{C}, \mathcal{C}') \propto \int d\boldsymbol{r} q(\boldsymbol{r}, \mathcal{C}, \mathcal{C}')$. The length scale ξ characterizes the two-point correlations of $q(\boldsymbol{r})$.

Figures 3(a)—3(c) illustrate the interpretation of the length scale ξ, over a range of $\langle Q \rangle$. In Fig. 3(c), $\langle Q \rangle$ is relatively large (strong pinning), and most of the system has high q, while small-q domains represent regions where the system differs from the reference state. As pinning is reduced, $\langle Q \rangle$ decreases [Fig. 3(b)], and more of the system is covered by small-q domains, with a characteristic length scale ξ (the situation is similar to the paramagnetic state of an Ising-like model). On further reducing $\langle Q \rangle$, [Fig. 3(a)] the small-q regions predominate, leaving behind high-q domains where configurations $\mathcal{C}$ and $\mathcal{C}'$ are similar, perhaps due to a particular property of the template in that area. Note that while Figs. 3(a)—3(c) represent systems over a range of c, they are all quite far from the limiting cases of strong pinning ($c \to 1$), where ξ is expected to be very small, and weak pinning ($c \to 0$), for which ξ is directly related to the radial distribution function $g(r)$ [33,36,38].

The key point [40] is that if the situation in Figs. 3(a)—3(c) holds, bimodal distributions $p(Q)$ will be found on considering finite systems of size $L \lesssim \xi$. The relevant distributions are sketched in Figs. 3(d)—3(f), and are similar to those in Figs. 2(a) and 2(b). Our results are, therefore, consistent with the inactive state having a correlation length $\xi \gtrsim L$. The SM includes results for four-point correlation functions, which reinforce this conclusion [45]. In plaquette models at low temperatures [33,44], the spacing between localized "excitations" [13,14] determines the length scale ξ. It has been proposed that a similar length scale determines the dynamical behavior of glasses formed by slow cooling [46]. Alternatively, the results of Fig. 2 are also consistent with the presence of a pinning-induced phase transition [11,12,42], in which case ξ would diverge. In the absence of a finite-size scaling analysis, we cannot distinguish these two scenarios, so we simply conclude that $\xi \gtrsim L$ for these inactive states.

To reinforce the connection between large domains and the results of Fig. 2, we recall the implications of a nonconvex effective potential $V(Q, c)$, which necessarily accompanies any bimodal distribution $p(Q|c)$. The potential is nonconvex if, for some Q, $(\partial^2/\partial Q^2)V(Q, c) < 0$. Hence, there exist two values of the overlap Q_1, Q_2 such that $V(Q_1) + V(Q_2) < 2V(Q_{\text{ave}})$, where $Q_{\text{ave}} = \frac{1}{2}(Q_1 + Q_2)$. Therefore, $p(Q_1)p(Q_2) > p(Q_{\text{ave}})^2$. This means that systems which are globally high- or low-q are more likely than systems where the domains are mixed, which implies that domain sizes ξ are comparable with the system size L [40]. We emphasize that this argument holds for finite systems, independently of the existence of any phase transition.

Finally, note that fluctuations of the overlap in these systems come from several sources: the choice of the reference configuration and of which particles to pin (the fixed "template"), and the thermal fluctuations associated with the configuration $\mathcal{C}_t$. The effect of pinning differs significantly between different templates: some are more likely to contribute to the large-Q peaks in Fig. 2, while others contribute more to the small-Q peak. In the picture of Figs. 3(a)—3(c), this implies that the high- or low-q regions of space are tied to specific locations in the system, depending on the structure of the template. However, on varying the choice of the frozen particles for a given reference configuration, we do not find any strong propensity for large Q or small Q. That is, the specific reference configuration does not strongly influence the locations of large-q or small-q domains.

We have shown that nonequilibrium states with low dynamical activity [16] have strong amorphous order, of a range ξ comparable with the system size $L = 5\sigma$. This order is much stronger than that found in equilibrium systems at the same temperature, consistent with the stability of the inactive states. The evidence for the large length scale ξ is indirect, but Fig. 3 shows how bimodal overlap distributions can be attributed to the existence of large domains. More generally, these results show how biased ensembles of trajectories [15,16] can be combined with static concepts such as effective potentials [39] and amorphous order [3–5], in order to understand stable glassy materials.

We thank Juan Garrahan, David Chandler, Ludovic Berthier, and Giulio Biroli for valuable discussions. This work was funded by the EPSRC through Grant No. EP/I003797/1.

[1] M. D. Ediger, C. A. Angell, and S. R. Nagel, J. Phys. Chem. **100**, 13200 (1996).
[2] P. G. Debenedetti and F. H. Stillinger, Nature (London) **410**, 259 (2001).
[3] J.-P. Bouchaud and G. Biroli, J. Chem. Phys. **121**, 7347 (2004).
[4] A. Montanari and G. Semerjian, J. Stat. Phys. **125**, 23 (2006).
[5] J. Kurchan and D. Levine, J. Phys. A **44**, 035001 (2011).
[6] G. Adam and J. H. Gibbs, J. Chem. Phys. **43**, 139 (1965).
[7] T. R. Kirkpatrick, D. Thirumalai, and P. G. Wolynes, Phys. Rev. A **40**, 1045 (1989).
[8] A. Cavagna, T. S. Grigera, and P. Verrocchio, Phys. Rev. Lett. **98**, 187801 (2007).
[9] G. Biroli, J.-P. Bouchaud, A. Cavagna, T. S. Grigera, and P. Verrocchio, Nat. Phys. **4**, 771 (2008).
[10] L. Berthier and W. Kob, Phys. Rev. E **85**, 011102 (2012).
[11] C. Cammarota and G. Biroli, Proc. Natl. Acad. Sci. U.S.A. **109**, 8850 (2012).
[12] W. Kob and L. Berthier, Phys. Rev. Lett. **110**, 245702 (2013).

[13] J. P. Garrahan and D. Chandler, Phys. Rev. Lett. **89**, 035704 (2002);J. P. Garrahan and D. Chandler, Proc. Natl. Acad. Sci. U.S.A. **100**, 9710 (2003).
[14] D. Chandler and J. P. Garrahan, Annu. Rev. Phys. Chem. **61**, 191 (2010).
[15] J. P. Garrahan, R. L. Jack, V. Lecomte, E. Pitard, K. van Duijvendijk, and F. van Wijland, Phys. Rev. Lett. **98**, 195702 (2007); J. P. Garrahan, R. L. Jack, V. Lecomte, E. Pitard, K. van Duijvendijk, and F. van WijlandJ. Phys. A **42**, 075007 (2009).
[16] L. O. Hedges, R. L. Jack, J. P. Garrahan, and D. Chandler, Science **323**, 1309 (2009).
[17] T. Speck and D. Chandler, J. Chem. Phys. **136**, 184509 (2012).
[18] T. Speck, A. Malins, and C. P. Royall, Phys. Rev. Lett. **109**, 195703 (2012).
[19] R. L. Jack, L. O. Hedges, J. P. Garrahan, and D. Chandler, Phys. Rev. Lett. **107**, 275702 (2011).
[20] R. L. Jack and J. P. Garrahan, Phys. Rev. E **81**, 011111 (2010).
[21] G. Biroli and J. P. Garrahan, J. Chem. Phys. **138**, 12A301 (2013).
[22] W. Kob and H. C. Andersen, Phys. Rev. E **51**, 4626 (1995); W. Kob and H. C. Andersen, Phys. Rev. E**52**, 4134 (1995).
[23] C. J. Fullerton and R. L. Jack, J. Chem. Phys. **138**, 224506 (2013).
[24] See Supplemental Material at http://link.aps.org/supplemental/10.1103/PhysRevLett.112.255701, including Refs. [25–27], for model details and further information on the effects of random pinning.
[25] P. Bolhuis, D. Chandler, C. Dellago, and P. Geissler, Annu. Rev. Phys. Chem. **53**, 291 (2002).
[26] J. D. Honeycutt and H. C. Andersen, J. Phys. Chem. **91**, 4950 (1987).
[27] H. Jonsson and H. C. Andersen, Phys. Rev. Lett. **60**, 2295 (1988).
[28] L. Berthier and W. Kob, J. Phys. Condens. Matter **19**, 205130 (2007).
[29] K. Kim, Europhys. Lett. **61**, 790 (2003).
[30] V. Krakoviack, Phys. Rev. E **82**, 061501 (2010).
[31] J. Kurzidim, D. Coslovich, and G. Kahl, J. Phys. Condens. Matter **23**, 234122 (2011).
[32] K. Kim, K. Miyazaki, and S. Saito, J. Phys. Condens. Matter **23**, 234123 (2011).
[33] R. L. Jack and L. Berthier, Phys. Rev. E **85**, 021120 (2012).
[34] S. Karmarkar and G. Parisi, Proc. Natl. Acad. Sci. U.S.A. **110**, 2752 (2013).
[35] B. Charbonneau, P. Charbonneau, and G. Tarjus, Phys. Rev. Lett. **108**, 035701 (2012).
[36] R. L. Jack and C. J. Fullerton, Phys. Rev. E **88**, 042304 (2013).
[37] G. M. Hocky, T. E. Markland, and D. R. Reichman, Phys. Rev. Lett. **108**, 225506 (2012).
[38] G. Szamel and E. Flenner, Europhys. Lett. **101**, 66005 (2013).
[39] S. Franz and G. Parisi, Phys. Rev. Lett. **79**, 2486 (1997).
[40] C. Cammarota, A. Cavagna, I. Giardina, G. Gradenigo, T. S. Grigera, G. Parisi, and P. Verrocchio, Phys. Rev. Lett. **105**, 055703 (2010).
[41] L. Berthier, Phys. Rev. E **88**, 022313 (2013).
[42] C. Cammarota, Europhys. Lett. **101**, 56001 (2013).
[43] R. L. Jack and J. P. Garrahan, J. Chem. Phys. **123**, 164508 (2005).
[44] C. Cammarota and G. Biroli, Europhys. Lett. **98**, 36005 (2012).
[45] See, for example, L. Berthier, G. Biroli, J.-P. Bouchaud, and R. L. Jack, in *Dynamical Heterogeneities in Glasses, Colloids, and Granular Media*, edited by L. Berthier, G. Biroli, J.-P. Bouchaud, L. Cipelletti, and W. van Saarloos, (Oxford University Press, New York, 2011), Chap. 2.
[46] A. S. Keys, J. P. Garrahan, and D. Chandler, Proc. Natl. Acad. Sci. U.S.A. **110**, 4482 (2013).